Merging the point clouds of the head and ear by using the iterative closest point method

Yan Luximon*
Nathaniel J Martin
Roger Ball
School of Design
The Hong Kong Polytechnic University
{sdtina, nathan.martin, sdroger}@polyu.edu.hk

Ming Zhang
Interdisciplinary Division of Biomedical Engineering
The Hong Kong Polytechnic University
ming.zhang@polyu.edu.hk

Abstract: Three dimensional (3D) surface body scanning technology has become an easy and rapid method for capturing the human shape. However, because most scanning systems rely on a direct line of sight, data is consistently missing in shadowed areas. When the head is scanned, data points at the back of the ear and the concha are consistently missing. To create an accurate head shape including the ear shape, the ear shape must be obtained separately. Efficiently merging the ear and head shapes is imperative before modelling and statistical analyses are performed. In this study, the ear and head shapes of the participants were obtained, and then the iterative closest point (ICP) method, a technique for aligning different objects in computer graphics, was applied to merge the ear and the corresponding head. This paper describes the principle and implementation of the procedure. The results indicated that the alignment error between the original ear from the head scan and the accurate ear was approximately 1.6 mm. The results of this study revealed that the method is beneficial to automatically aligning human 3D point cloud data accurately and efficiently. This method can be used for creating an accurate head and ear model for head- and face-related product design.

Keywords: Computer-aided design, image analysis, digital human model, 3D human model, human head and ear

1 Introduction

With the invention of three dimensional (3D) body scanning technologies, studies on human shape based on scanned databases have developed rapidly during the last few decades. On the basis of the scanning data, human 3D shapes, including head, body, and foot shapes, have been studied and modelled by researchers (Wang et al., 2003; Luximon and Goonetilleke, 2004; Zhang and Molenbroek, 2003; Azouz et al., 2006). Human modelling can be applied widely in areas including medical equipment, helmet, clothing, and shoes.

Although using 3D body scanning technology is easy and rapid, limitations exist (Luximon et al., 2011). Most of the current 3D scanning devices are governed by the principles of optics, because many such devices use laser or other optical methods. Thus, these scanners cannot capture data in shadowed areas of an object, resulting in missing data points. In addition, the scanning results are affected by ambient lighting levels (Luximon and Goonetilleke, 2004). When the missing or noise areas are small, the data can be corrected according to interpolation methods; however, large missing regions cannot be accurately filled. This is particularly obvious during head scans. A human face can be clearly captured in a head scan, but the data for the concave area and area behind the ears are consistently missing. Reichinger et al. (2013) compared various methods of scanning human ears, and discussed difficulties to scan living ears such as long scanning duration and poorer accuracy comparing to scanning plaster ears. Although studies have been conducted on traditional anthropometric manual measures for obtaining the ear dimensions (Farkas, 1994; Liu, 2008; Ismaila, 2009; Alexander, 2011), more accurate 3D ear data are needed for designing ear-related products, such as eyewear, headphones, and hearing aids.

To compensate for the missing ear data, conventional casting methods can be applied to ascertain ear shapes (Kouchi and Mochimaru, 2004). Although accurate ear data are essential for ear-related products, use of such data is impractical for ear and head related products unless the two datasets (ear and head) are merged. Although the data can be merged manually, such a process is tedious. The iterative closest point (ICP) is a technique for preprocessing and aligning two dimensional (2D) images and 3D shapes (Besl and McKay, 1992). In the fields of computer vision and graphics, the ICP method is used for recognising 3D patterns, registering shapes, and matching 3D shapes (Zhang 1994; Rusinkiewicz and Levoy, 2001; Jost and Hügli, 2002; Rusinkiewicz et al., 2003; Guo et al., 2014). Digital human data with inherently wide shape variations poses challenges in data acquisition and model building (Luximon and Goonetilleke, 2004). Some researchers have applied the method in human recognition (Cook et al., 2004; Islam et al., 2008; ter Haar and Veltkamp, 2010; Yan and Bowyer, 2007). Harder et al. (2013) used the method in merging the children's multiple head scans but accuracy were not discussed in detail. This study applied the ICP technique to combine the head and ear shapes from different methods of data acquisition, assessing the implementation and accuracy of the ICP procedure in digital human-related data.

2 Methodology

2.1 Scan data collection

Ten Chinese adults participated in the data collection. The head shapes of participants were first scanned using a high resolution Cyberware 3030 3D colour laser scanner. Individual 3D head shape data were collected in approximately 17 seconds (Figure 1(a)). Because the scanner uses laser technology, the data at the back region of both ears were almost missing completely (Figure 1(b)). The holes were filled using interpolation methods; thus, the generated ear shape was inaccurate and inappropriate for design (Figure 1(c)).

Figure 1 Sample of (a) Head scan (b) Enlarged ear region with holes (c) Ear region with holes filled

(a) (b) (c)

The ear shapes were later obtained using the conventional casting method. A negative mould was developed using a mixture of Blueprint® cremix alginate powder (Dentsply International) and water. After the mixture set, the mould was removed and formed into a plaster cast (Figure 2). When the plaster casts had dried, a highly accurate Scan 3D II laser scanner was used to scan the ear casts. To avoid missing data, each ear cast was scanned several times from various angles. Although complete ear data can be obtained using different methods, this study used Rapidform software to combine the data from different views into one file. All ear shapes were obtained from the participants after they underwent head scanning.

Figure 2 Sample of ear cast

2.2 Problem formulation

After data collection, the original head scan (*H*) and ear scan (*E*) datasets were obtained. Assume that the set H_E represents the data point cloud of the ear from head scan *H*, and E_C represents the data point cloud of the ear from ear cast data *E*.

The algorithm merges the ear data from ear cast E_C into the point cloud data of head scan H_E. In other words, the objective is determining the optimal rotation (M_R) and transformation matrices (M_T) to align E_C near H_E. Therefore, H_E was set as the model shape and $\hat{f}(E_C)$ was set as the aligned shape.

The problem formulation is learning the optimal function $\hat{f} \in F$, where F is a mapping function for the ear shape dataset, which is mapped from sample space *S* (ear coordinate system) into feature space *Φ* (head coordinate system) (Figure 3). The sample space *S* and feature space *Φ* are elements of R^3 (Equation (1)). Let E_C be the ear shape dataset in the sample space *S* and the mapping function $\hat{f}(E_C)$ be a function of E_C, rotation matrix ($M_R \in R^{3\times3}$), and translation matrix ($M_T \in R^{3\times1}$) (Equation (2)). The mapping function $\hat{f}(E_C)$ represents the minimisation of the error of the given mapping of the model shape.

$$\text{Let } f : S \in R^3 \rightarrow \Phi \in R^3 \qquad (1)$$

$$\hat{f}(E_C) := M_R E_C + M_T \in \Phi \qquad (2)$$

Figure 3 Mapping the ear dataset from the sample space into the feature space

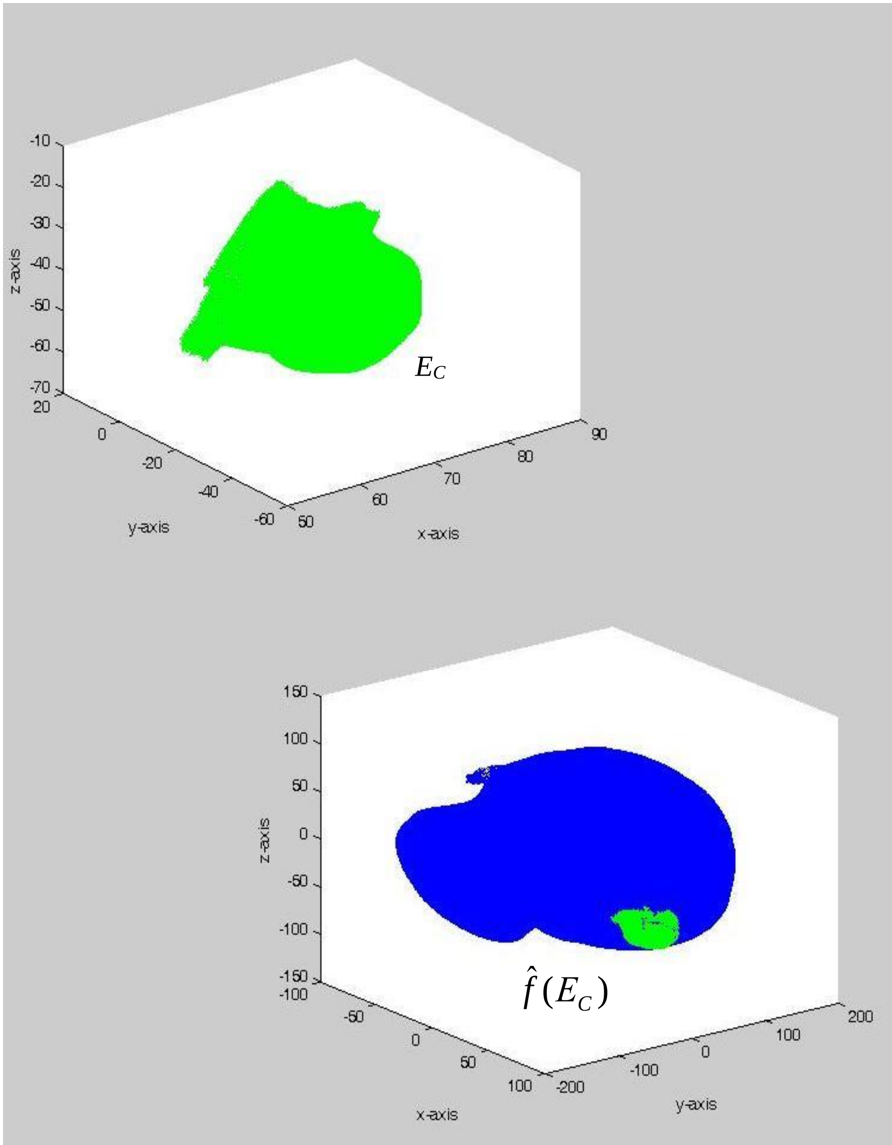

The ICP method (Besl and McKay, 1992) was used to find $\hat{f}$ for merging two datasets. $ICP(\cdot,\cdot)$ is a function of the model shape (the incomplete ear from the head scan H_E) and the dataset that must be aligned (the complete ear scan E_C) (Equation (3)).

$$\hat{f}(E_C) \approx ICP(H_E, E_C) \quad (3)$$

$$d(H_E, \hat{f}(E_C)) := \min_{p_{HE} \in H_E} \| p_{HE} - p_{EC} \| \text{ for } \forall i \text{ and } \forall j, \quad (4)$$

where $p_{HE} = (x_{HEi}, y_{HEi}, z_{HEi}) \in H_E$, $p_{EC} = (x_{ECj}, y_{ECj}, z_{ECj}) \in \hat{f}(E_C)$

$$d(p_i, p_j) = \| p_i - p_j \| = \sqrt{(x_j - x_i)^2 + (y_j - y_i)^2 + (z_j - z_i)^2} \quad (5)$$

$$H_{merged} := H \cup \hat{f}(E_C) - H_E \quad (6)$$

The ICP algorithm minimises the distance metric (or Euclidean norm) of the two datasets. The distance metric d, from H_E to $\hat{f}(E_C)$ uses H_E to calculate the distance (Equation (4)). The equation $d(\hat{f}(E_C), H_E) := \min_{p_{EC} \in E_C} \| p_{EC} - p_{HE} \|$ yields slightly different results from those of $d(H_E, \hat{f}(E_C))$ because the reference shape is different. The distance between two data points is calculated using Equation (5). After the optimal M_R and M_T are found (Equation (2)), denoted as $\tilde{M}_R$ and $\tilde{M}_T$, respectively, the point cloud data of the head scan H and $\hat{f}(E_M)$ are combined into one dataset H_{merged} by using Equation (6).

2.3 Algorithm

2.3.1 Initial estimation of H_E and E_C

According to the problem formulation, the ear shape data from the head scan (H_E) and from the cast (E_C) must be selected. For the ear cast data (E) (Figure 4(a)), the supports were manually and digitally deleted and the ear data points were aligned to approximately match the coordinate system of the head scan (Figure 4(b)) and create dataset E_C. The centre of the ear in the casting $(\overline{x_{EC}}, \overline{y_{EC}}, \overline{z_{EC}})$ is calculated using the mean of Cartesian coordinates (x, y, z) of all date points in dataset E_C.

To select H_E from H (Figure 5(a)), first, an approximate centre of the ear was manually located. The centre of the ear in the head scan is at $(\overline{x_{HE}}, \overline{y_{HE}}, \overline{z_{HE}})$. A region $(\overline{x_{HE}} \pm \partial, \overline{y_{HE}} \pm \partial, \overline{z_{HE}} \pm \partial)$ was selected to consider the data points surrounding the ear centre. If ∂ = 50 mm, then the ear shape from the head scan is within the extracted shape (Figure 5(b)). Larger ∂ values can be used but slow the programme, whereas smaller ∂ values might not enable selecting the complete ear shape. The initial estimate of the dataset for H_E is denoted as H_{E0}.

Figure 4 Ear scan (a) Ear cast dataset E (b) Ear dataset from ear cast E_C

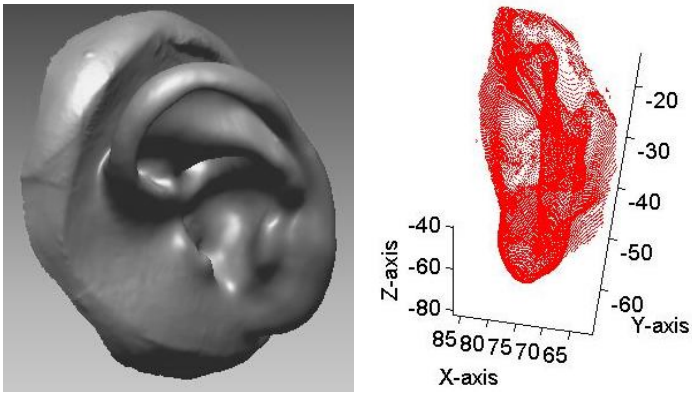

(a) (b)

Figure 5 Head scan (a) Head scan dataset H (b) First estimate of ear dataset from head scan H_{E0}

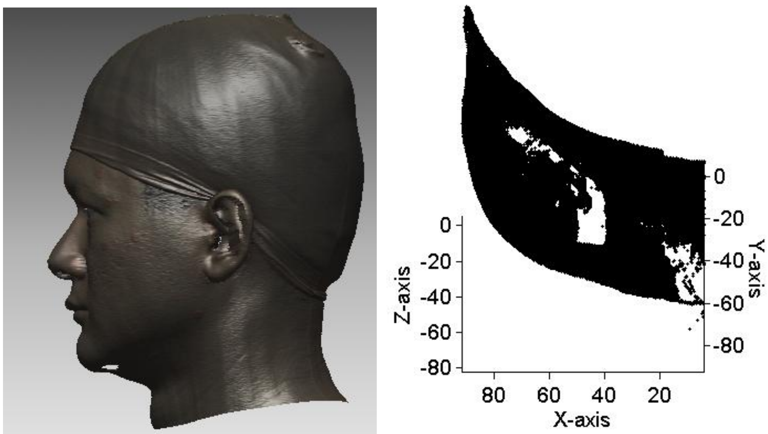

(a) (b)

2.3.2 Second estimation of H_E

The centre point ($\overline{x_{EC}}$, $\overline{y_{EC}}$, $\overline{z_{EC}}$) of dataset E_C was translated to the centre point ($\overline{x_{HE}}$, $\overline{y_{HE}}$, $\overline{z_{HE}}$) of the dataset H_{EO} (Figure 6). By using all points in dataset E_C, the shortest distance from E_C to H_{EO} was calculated. Equations similar to Equations (4) and (5) were used. In addition, the points in dataset H_{EO}, in which the shortest distance occurs, were recorded. This dataset was denoted as H_{E1}, where $H_{E1} \subset H_{E0}$. Figure 7 shows the dataset H_{E1}.

Figure 6 Initial alignment of H_{E0} and E_C

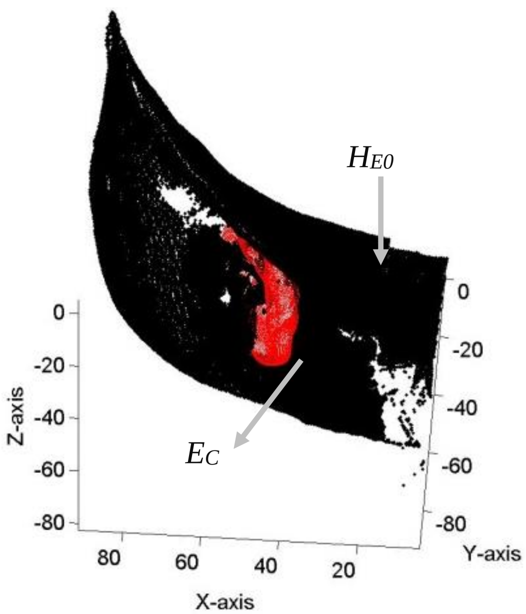

Figure 7 Selected datasets for H_E (H_{E1}) and E_C

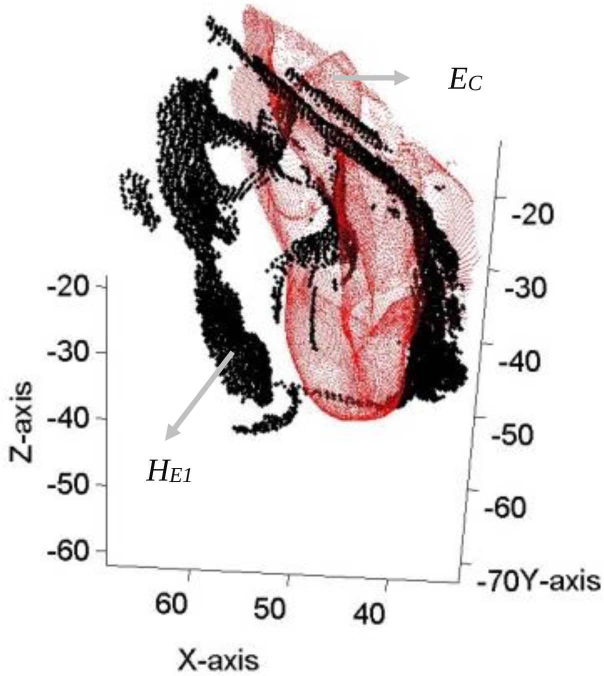

2.3.3 ICP algorithm implementation

After selecting the head scan (H_{E1}) and ear scan (E_C) datasets, the ICP method (Besl and McKay, 1992) was used for aligning these two sets of data point clouds. The dataset H_{E1} more favourably represented the ear dataset from the head scan (H_E) and was hence used in the ICP algorithm with the dataset E_C according to Equation (3). All programmes were written in MATLAB. The ICP code is based on Bergström (2007) MATLAB codes. This ICP algorithm uses a Delaunay tessellation of model points, fitting the data points to the model points. The fit is based on minimization of the sum of square of errors with the closest model and data points. Figure 8 shows the alignment after the ICP procedure was applied.

Figure 8 H_{E1} and E_C alignment by using the ICP method

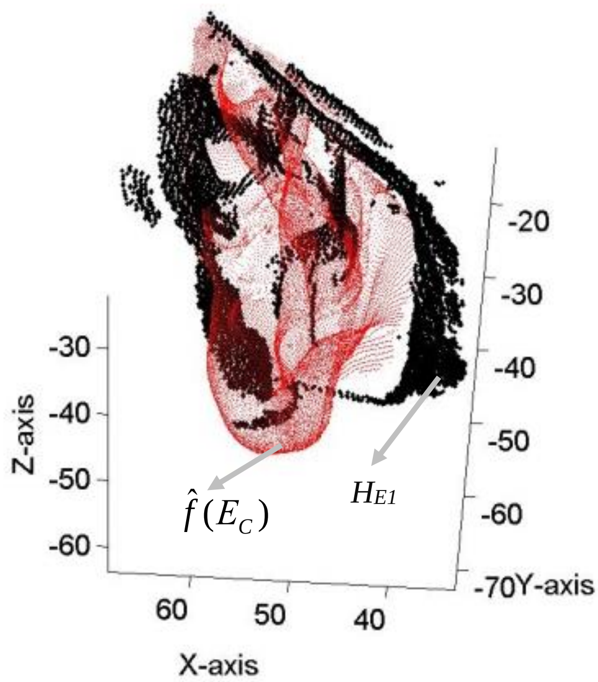

3 Results

3.1 Error estimation result

Figure 6 shows the result of the initial alignment between the ear data from the head scan (H_{E0}) and ear cast (E_C). The minimum error (*d*) from each point of dataset E_C to that of dataset H_{E0} was calculated. Table 1 lists the minimum (Min), maximum (Max), average (Mean), and standard deviation (SD) values of the error *d*. The mean of maximum error was 13.20 mm for the right ear and 15.17 mm for the left ear.

The results showed that the error was large after the initial alignment. Dataset H_{E1} was calculated as discussed previously (Figure 7). The minimum error (*d*) from each point of dataset E_C to each point of dataset H_{E1} was the same (Table 1). Table 2 displays the minimum error (*d*) calculated from each point of dataset H_{E1} to each point of dataset E_C. The mean of maximum error was 10.27 mm for the right ear and 11.23 mm for the left ear.

Table 1 Minimum (Min), maximum (Max), average (Mean), and standard deviation (SD) values of the error *d* from E_C to H_{E0}

	Right				Left			
Subject Number	Min	Max	Mean	SD	Min	Max	Mean	SD
1	0.07	13.26	4.59	2.32	0.06	14.07	5.05	1.97
2	0.09	11.98	5.86	2.54	0.08	13.12	5.60	2.41
3	0.05	12.02	5.50	2.71	0.04	14.41	6.22	3.26
4	0.03	14.20	6.02	3.23	0.03	12.50	5.88	2.68
5	0.05	12.14	4.86	2.51	0.07	13.02	5.97	2.73
6	0.03	14.56	6.32	2.96	0.05	14.82	6.26	2.64
7	0.05	15.47	5.67	2.60	0.03	14.40	5.47	2.43
8	0.08	10.59	4.81	2.10	0.06	22.20	5.07	2.19
9	0.04	14.88	6.20	2.86	0.05	12.60	5.77	2.34
10	0.07	12.94	6.72	2.77	0.08	20.55	6.51	3.04
Mean	0.06	13.20	5.66	2.66	0.05	15.17	5.78	2.57
SD	0.02	1.55	0.71	0.32	0.02	3.39	0.49	0.39

Table 2 Minimum (Min), maximum (Max), average (Mean), and standard deviation (SD) values of the error *d* from H_{E1} to E_C

	Right				Left			
Subject Number	Min	Max	Mean	SD	Min	Max	Mean	SD
1	0.03	8.01	2.62	1.50	0.03	8.92	2.59	1.69
2	0.01	9.95	3.73	2.15	0.03	11.42	3.42	1.96
3	0.05	11.14	4.04	2.27	0.02	11.57	4.45	2.57
4	0.02	12.93	4.44	2.54	0.02	9.18	3.59	1.84
5	0.02	9.27	2.51	1.55	0.04	11.34	4.21	2.33
6	0.04	9.31	3.27	1.95	0.01	10.35	3.13	1.94
7	0.03	10.09	3.32	2.00	0.04	10.81	2.91	1.65
8	0.02	8.89	2.87	1.76	0.04	17.17	3.02	1.84
9	0.06	11.84	4.72	2.45	0.03	9.92	2.93	1.74
10	0.01	11.26	3.69	1.97	0.03	11.61	3.75	2.13
Mean	0.03	10.27	3.52	2.01	0.03	11.23	3.40	1.97
SD	0.02	1.50	0.74	0.35	0.01	2.30	0.60	0.30

The ICP method was applied to H_{E1} and E_C (Figure 8). The distance error was calculated from H_{E1} to $\hat{f}(E_C)$. Table 3 shows that the mean of maximum error was 7.05 mm for the right ear and 8.29 mm for the left ear.

Table 3 Minimum (Min), maximum (Max), average (Mean), and standard deviation (SD) values of the error d from H_{E1} to $\hat{f}(E_C)$

	Right				Left			
Subject Number	Min	Max	Mean	SD	Min	Max	Mean	SD
1	0.03	5.86	1.46	0.93	0.03	6.90	1.11	0.87
2	0.01	8.68	1.95	1.92	0.03	8.62	1.38	1.30
3	0.05	5.97	1.58	1.17	0.02	8.16	1.74	1.32
4	0.02	5.48	1.60	1.05	0.02	7.42	2.02	1.74
5	0.02	6.43	1.30	0.91	0.04	8.47	2.05	1.97
6	0.04	9.44	1.45	1.12	0.01	4.13	1.09	0.74
7	0.03	5.91	1.64	1.18	0.04	10.79	1.63	1.10
8	0.02	6.60	1.36	1.00	0.04	12.88	1.28	1.20
9	0.06	9.45	2.36	2.09	0.03	10.18	1.27	1.22
10	0.01	6.65	1.84	1.41	0.03	5.29	1.73	1.19
Mean	0.03	7.05	1.65	1.28	0.03	8.29	1.53	1.27
SD	0.02	1.54	0.32	0.41	0.01	2.58	0.35	0.36

3.2 Comparison to manual method

To compare the accuracy of the ICP method and manual method, the ear dataset E_C of each participant was manually aligned with dataset H_{E1}. The distance error was calculated from H_{E1} to manually aligned E_C. Table 4 shows that the mean of maximum error was 9.35 mm for the right ear and 9.95 mm for the left ear. Results showed that the ICP method provided less distance error than the manual method.

Table 4 Minimum (Min), maximum (Max), average (Mean), and standard deviation (SD) values of the error *d* from H_{E1} to manually aligned E_C

	Right				Left			
Subject Number	Min	Max	Mean	SD	Min	Max	Mean	SD
1	0.04	10.02	2.42	1.78	0.02	10.03	2.06	1.95
2	0.03	9.28	2.09	1.38	0.03	10.05	2.00	1.69
3	0.02	9.18	2.39	1.97	0.01	8.82	2.42	2.01
4	0.02	9.53	2.22	1.61	0.02	8.90	2.14	1.67
5	0.02	9.48	1.95	1.44	0.02	9.00	1.84	1.42
6	0.02	9.75	2.54	2.27	0.01	9.61	2.39	2.01
7	0.02	8.23	1.89	1.95	0.02	8.26	2.00	1.83
8	0.03	7.49	2.39	1.54	0.04	14.10	2.36	1.81
9	0.02	10.04	2.49	2.18	0.02	10.07	2.36	2.12
10	0.03	10.54	2.50	2.20	0.02	10.64	2.58	2.16
Mean	0.03	9.35	2.29	1.83	0.02	9.95	2.22	1.87
SD	0.01	0.90	0.24	0.33	0.01	1.63	0.24	0.23

3.3 Merged model

The complete head dataset including the ears was created after H_{merged} was calculated. Figure 9(a) depicts an example of the surface result generated using a 3D point cloud dataset. Figures 9(b) and 9(c) illustrate the complete head and ear shape model from different views.

Figure 9 Example of the merged model in (a) Point cloud data (b) Front view (c) Back view

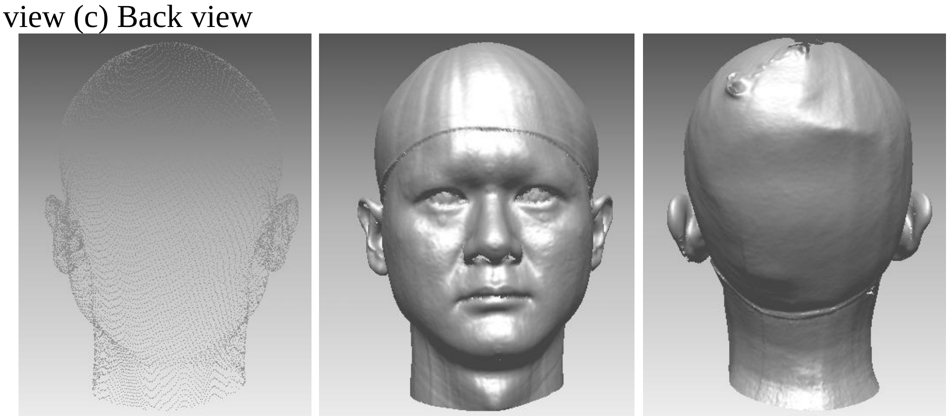

(a) (b) (c)

4 Discussion and conclusion

Although 3D scanning technologies and human modelling research have been applied and performed widely, previous studies have not provided highly accurate 3D shapes of the head and ears. Comparisons of different scanning methods showed that scanning living ears is difficult and time consuming (Reichinger et al., 2013). Although ear shapes are particularly difficult to render accurately, they are crucial for designing products such as hearing aids and in studies such as ear surgery simulations. To create a complete dataset of head and ear shapes, a combination of the conventional cast technique and 3D scan technology was adopted in this study. Designers and industries can use these datasets to design well-fitting ear-related products innovatively and easily.

The ICP method was applied in this study to merge head scan and ear cast datasets. The head scan had missing data points at the ear region that were replaced by the ear cast dataset. The results revealed that the two datasets were combined with a 1.6-mm distance error on average. Although software including Rapidform, MeshAlign, and MeshMerge can be used to align and merge 3D scans, these software packages are semiautomatic (ter Haar et al., 2005) and require manual operation for selecting corresponding points. In addition, such software packages may not be useful for batch processing of numerous datasets from anthropometric studies. In the present study, the ICP method required no landmarks during data processing. The entire alignment process was computed automatically, and data from multiple participants were analysed using MATLAB programmes. Furthermore, the method was used to manage the point cloud data directly; it is swifter and easier than manual operation. Results also demonstrated that the ICP method had higher accuracy than the manual method.

However, the ICP process also has drawbacks. The alignment error between the head scan and ear cast can be affected by head movement during the head scanning and ear casting processes. Therefore, the alignment results of merging two datasets varied individually. The measurement error is typically large when human subjects are involved because of wide variation of human shapes, deformations of the soft tissue surface, and possible hair influence. Better performance head scanner with multiple cameras could increase the data points at ear area and achieve higher alignment accuracy. Future studies can focus on improving these drawbacks.

Acknowledgement

This study was made possible through the support from the Hong Kong Polytechnic University (A-PM10).

References

Alexander, K.S. (2011) 'A morphometric study of the human ear', *Journal of Plastic, Reconstructive & Aesthetic Surgery*, Vol. 64, No. 1, pp. 41-47.

Azouz, Z.B., Rioux, M., Shu, C. and Lepage, R. (2006) 'Characterizing human shape variation using 3D anthropometric data', *The Visual Computer*, Vol. 22, No. 5, pp. 302-314.

Bergström, P. (2007) 'Iterative Closest Point Method', Ref number: 12627, file name "icp.m", Matlab central file exchange (www.mathworks.com).

Besl, P.J. and McKay, N.D. (1992) 'A method for registration of 3-D shapes', *IEEE Trans. on Pattern Analysis and Machine Intelligence*, Vol. 14, No. 2, pp. 239-256.

Cook, J., Chandran, V. Sridharan, S. and Fookes, C. (2004) 'Face recognition from 3D data using Iterative Closest Point algorithm and Gaussian mixture models', Proceedings. 2nd International Symposium on 3D Data Processing, Visualization and Transmission, (3DPVT 2004), pp.502-509.

Farkas, L.G. (1994) *Anthropometry of the head and face*, Raven Press, New York: USA.

Guo, Y., Sohel, F., Bennamoun, M., Wan, J. and Lu, M. (2014) 'An Accurate and Robust Range Image Registration Algorithm for 3D Object Modeling', *IEEE Transactions on Multimedia*, Vol. 16, No. 5, pp. 1377-1390.

Harder, S., Paulsen, R.R., Larsen M. and Laugesen, S. (2013) 'A three dimensional children head database for acoustical research and Development', in *Proceedings of Meetings on Acoustics*, ICA 2013 Montreal, Canada.

Jost, T. and Hügli, H. (2002) 'Fast ICP algorithms for shape registration Pattern Recognition', in lecture Notes in Computer Science, Vol. 2449, pp. 91-99.

Kouchi M. and Mochimaru M. (2004) ‘Analysis of 3D face forms for proper sizing and CAD of spectacle frames’, *Ergonomics*, Vol. 47, No. 14, pp. 1499-1516.

Islam, S.M.S., Bennamoun, M., Mian A.S. and Davies, R. (2008) ‘A Fully Automatic Approach for Human Recognition from Profile Images Using 2D and 3D Ear Data’, in *Proceedings of 3DPVT'08 - the Fourth International Symposium on 3D Data Processing, Visualization and Transmission*, Atlanta, GA, USA.

Ismaila, O.S. (2009) ‘Anthropometric Data of Hand, Foot and Ear of University Students in Nigeria’, *Leonardo Journal of Sciences*, Vol. 15, pp. 15-20.

Liu, B.S. (2008) ‘Incorporating anthropometry into design of ear-related products’, *Applied Ergonomics*, Vol. 39, No. 1, pp. 115-121.

Luximon, A. and Goonetilleke, R.S. (2004) ‘Foot shape modeling’, *Human Factors*, Vol. 46, No. 2, pp.304-315.

Luximon, Y., Ball, R., and Justice, L. (2011) ‘The 3D Chinese head and face modeling’, *Computer-Aided Design*, Vol. 44, No. 1, pp. 40-47.

Reichinger, A., Majdak, P., Sablatnig, R. and Maierhofer, S. (2013) ‘Evaluation of Methods for Optical 3-D Scanning of Human Pinnas’, *2013 International Conference on 3D Vision*, Seattle, USA.

Rusinkiewicz, S., Levoy, M., Gelfand, N. and Ikemoto, L. (2003) ‘Geometrically stable sampling for the ICP algorithm’, in *Proceedings of Fourth International conference on 3D digital imaging and modeling*, October 2003, Banff Canada.

Rusinkiewicz, S. and Levoy, M. (2001) ‘Efficient variants of the ICP algorithm’, in *Proceedings of Third International conference on 3D digital imaging and modeling*, Quebec City, Que, pp. 145-152.

ter Haar, F.B., Cignoni, P., Min, P. and Veltkamp, R.C. (2005) ‘A comparison of systems and tools for 3D scanning’, in *3D Digital Imaging and Modeling: Applications of Heritage, Industry, Medicine and Land Workshop*, Padova, Italy, Session P.12.

ter Haar, F.B. and Veltkamp, R.C. (2010) ‘Expression modeling for expression-invariant face recognition’, *Computers & Graphics*, Vol. 34, No. 3, pp. 231-241.

Wang, C.C.L., Chang, T.K.K. and Yuen, M.M.F. (2003) ‘From laser-scanned data to feature human model: a system based on fuzzy logic concept’, *Computer-Aided Design*, Vol. 35, pp. 241–253.

Yan, P. and Bowyer, K.W. (2007) 'Biometric Recognition Using 3D Ear Shape', *IEEE Transactions on pattern analysis & machine intelligence*, Vol. 29, No. 8, pp. 1297-1308.

Zhang, B., Molenbroek, J.F.M. (2004) 'Representation of a human head with bi-cubic B-splines technique based on the laser scanning technique in 3D surface anthropometry', *Applied Ergonomics*, Vol. 35, No. 5, pp. 459–465.

Zhang, Z. (1994) 'Iterative point matching for registration of free-form curves and surfaces', *International Journal of Computer Vision*, Vol. 13, No. 2, pp. 119–152.